Compile Scene Graphs with Reinforcement Learning

Zuyao Chen[1, 2] **Jinlin Wu**[3, 4] **Zhen Lei**[3, 4] **Marc Pollefeys**[2, 5] **Chang Wen Chen**[1]
[1]The Hong Kong Polytechnic University [2]ETH Zürich [3]CAIR, HKISI-CAS
[4]Institute of Automation, CAS [5]Microsoft

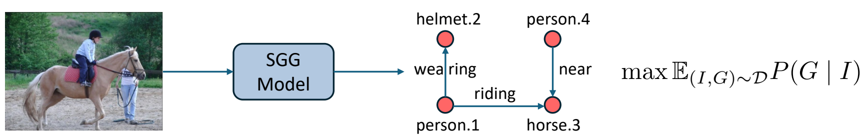

(a) Traditional SGG methods directly maximize the expectation of the likelihood $\mathbb{E}_{(I,G)\sim\mathcal{D}} P(G \mid I)$, where image-graph pairs (I, G) are sampled from the dataset $\mathcal{D}$.

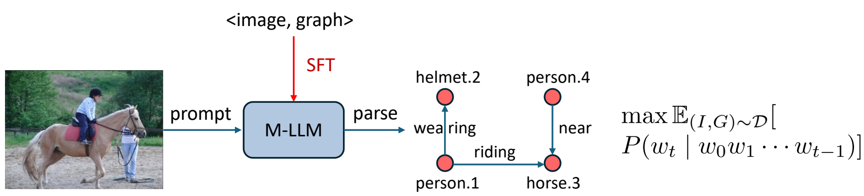

(b) M-LLM with SFT is optimized token by token (here, w_i refers to a token).

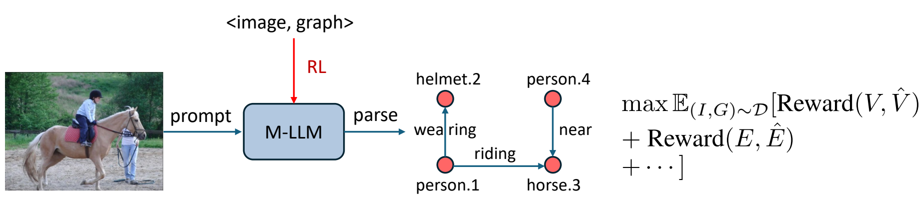

(c) M-LLM with RL is optimized using rule-based rewards. Here, $G = (V, E)$ and $\hat{G} = (\hat{V}, \hat{E})$ refer to the ground-truth and predicted scene graphs, respectively.

Figure 1: Comparison of traditional Scene Graph Generation (SGG), multimodal LLMs (M-LLMs) with supervised fine-tuning (SFT), and M-LLMs with reinforcement learning (RL) for SGG.

Abstract

Next token prediction is the fundamental principle for training large language models (LLMs), and reinforcement learning (RL) further enhances their reasoning performance. As an effective way to model language, image, video, and other modalities, the use of LLMs for end-to-end extraction of structured visual representations, such as scene graphs, remains underexplored. It requires the model to accurately produce a set of objects and relationship triplets, rather than generating text token by token. To achieve this, we introduce *R1-SGG*, a multimodal LLM (M-LLM) initially trained via supervised fine-tuning (SFT) on the scene graph dataset and subsequently refined using reinforcement learning to enhance its ability to generate scene graphs in an end-to-end manner. The SFT follows a conventional prompt-response paradigm, while RL requires the design of effective reward signals. Given the structured nature of scene graphs, we design a graph-centric reward function that integrates node-level rewards, edge-level rewards, and a format

Preprint. Under review.

consistency reward. Our experiments demonstrate that rule-based RL substantially enhances model performance in the SGG task, achieving a zero failure rate—unlike supervised fine-tuning (SFT), which struggles to generalize effectively. Our code is available at `https://github.com/gpt4vision/R1-SGG`.

1 Introduction

Scene graphs, as structured visual representations, have gained increasing attention in many vision applications, such as robot manipulation [Zhu *et al.*, 2021; Zhang *et al.*, 2025], robot navigation [Gu *et al.*, 2024; Miao *et al.*, 2024; Yin *et al.*, 2024], and medical image/video analysis [Lin *et al.*, 2022; Özsoy *et al.*, 2022], *etc*. To generate scene graphs from an image, traditional Scene Graph Generation (SGG) models [Johnson *et al.*, 2015; Xu *et al.*, 2017; Li *et al.*, 2017; Zellers *et al.*, 2018; Tang *et al.*, 2019; Chen *et al.*, 2019; Li *et al.*, 2022a; Khandelwal and Sigal, 2022; Cong *et al.*, 2023; Zhang *et al.*, 2023; Chen *et al.*, 2024] decouple the task into two subtasks, *i.e.*, object detection and visual relationship recognition, and directly maximize the likelihood of the ground-truth labels given the image (Fig. 1 (a)). Essentially, these models tend to overfit the distribution of annotated datasets; consequently, they struggle to handle long-tail distributions and are prone to generating biased scene graphs (*e.g.*, all predicted relationships are head classes like "on" and "of").

While traditional SGG models rely on manual annotated datasets and struggle to generalize to new domains, recent advances in large languge models (LLMs) offer a new paragdim. LLM4SGG [Kim *et al.*, 2023] utilizes an LLM to extract relationship triplets from captions using both original and paraphrased text, while GPT4SGG [Chen *et al.*, 2023] employs an LLM to synthesize scene graphs from dense region captions. Additionally, Li [Li *et al.*, 2024] generates scene graphs via image-to-text generation using vision-language models (VLMs). These weakly supervised methods demonstrate potential for generating scene graphs with little or no human annotation but suffer from accuracy issues in the generated results.

Despite these advancements, existing methods typically employ text-only LLMs or rely on intermediate captions as input, which may not fully leverage the rich visual context. In contrast, multimodal large language models (M-LLMs) which integrate both visual and linguistic modalities offer the potential for more direct and holistic scene understanding. By processing visual information alongside natural language prompts, M-LLMs can generate scene graphs in an end-to-end manner. However, in practice, M-LLMs suffer from instruction following (*e.g.*, the output does not contain "objects" or "relationships"), repeated response (*e.g.*, "objects":[... "id": "desk.9", "bbox": [214, 326, 499, 389], "id": "desk.10", "bbox": [214, 326, 499, 389], "id": "desk.11", "bbox": [214, 326, 499, 389], ...]), inaccurate location, *etc*. These challenges highlight the need for better alignment between visual understanding and structured representation within the M-LLM framework.

To improve instruction-following and structured output generation in M-LLMs, one intuitive solution is to perform Supervised Fine-tuning (SFT) on scene graph datasets (see Fig. 1) (b)). In the context of SGG, SFT aligns the model's outputs with expected formats (*e.g.*, structured lists of objects and relationships) by training it on high-quality scene graph annotations. This process encourages the model not only to recognize entities and relations from the image but also to organize them into a coherent and valid graph structure. Nevertheless, SFT alone may still be insufficient as all output tokens are weighted equally in the loss. For example, the experimental results on the VG150 dataset Xu *et al.* [2017] reveal that even with SFT, M-LLM still has a high failure rate to generate a valid and high-quality scene graph. The drawback of SFT in SGG lies in the lack of effective signals to correct the output (*e.g.*, the model cannot directly utilize the Intersection over Union (IoU) between the predicted box and the ground truth to refine its output).

To advance M-LLMs for effective Scene Graph Generation (SGG), we propose *R1-SGG*, a novel framework leveraging visual instruction tuning enhanced by reinforcement learning (RL). The visual instruction tuning stage follows a conventional supervised fine-tuning (SFT) paradigm, *i.e.*, fine-tuning the model using prompt-response pairs with a cross-entropy loss. For the RL stage, we adopt GRPO, an online policy optimization algorithm introduced in DeepSeekMath Shao *et al.* [2024].

To effectively apply GRPO to the SGG task, we introduce several rule-based rewards, reflecting key characteristics of scene graphs. Generally, given an image and an associated textual prompt, the multimodal LLM generates a set of predicted objects and relationship triplets. To establish a precise node-level correspondence between the predicted set and the ground-truth annotations, we formulate this alignment problem as a bipartite matching problem, efficiently resolved using the Hungarian algorithm [Kuhn, 1955]. Upon solving the bipartite matching, we acquire an optimal mapping between predicted nodes and ground-truth nodes. The rewards are then systematically computed as follows: 1) **Node-level reward**: Calculated as the embedding similarity between the predicted object and the corresponding ground-truth object, combined with the Intersection-over-Union (IoU) of their bounding boxes. 2) **Edge-level reward**: Measured by the embedding similarity of the predicted predicate and the ground-truth predicate associated with matched object pairs, reflecting the accuracy of relationship predictions. This graph-centric reward design along with a format reward (*e.g.*, the output should contain "objects" and "relationships") effectively guides the policy optimization process to refine the model for generating accurate, contextually consistent, and diverse scene graphs.

Our contributions can be summarized as follows

- We explore how to develop a multimodal LLM for Scene Graph Generation (SGG), by leveraging visual instruction tuning with reinforcement learning (RL). To our knowledge, this is a pioneer work that develop a multimodal LLM to generate scene graphs in an end-to-end manner.
- Graph-centric, rule-based rewards are designed to guide policy optimization in a manner aligned with standard evaluation metrics in SGG, such as the recall of relationship triplets—metrics that cannot be directly optimized through SFT.
- Experimental results demonstrate that the proposed framework improves the ability to understand and reason about scene graphs for multimodal LLMs.

2 Related Work

Scene Graph Generation (SGG). Scene Graph Generation (SGG) is a foundational task in structured visual understanding, where the goal is to represent an image as a graph of objects and their pairwise relationships. Traditional approaches like Xu *et al.* [2017]; Li *et al.* [2017]; Zellers *et al.* [2018]; Tang *et al.* [2019]; Chen *et al.* [2019]; Li *et al.* [2022a]; Khandelwal and Sigal [2022]; Cong *et al.* [2023] decouple the task into object detection and relationship classification stages, and are typically trained via supervised learning on datasets such as Visual Genome (VG150) [Xu *et al.*, 2017]. While effective, these models are limited by their reliance on annotated data and exhibit strong bias toward head predicates such as "on" or "of", struggling on long-tail classes.

To overcome the closed-set limitation, recent work has explored open-vocabulary SGG. For example, OvSGTR [Chen *et al.*, 2024] extends scene graph prediction to a fully open-vocabulary setting by leveraging visual-concept alignment. In parallel, weakly supervised methods have been developed to reduce the annotation burden. These approaches, such as those proposed by Zhong *et al.* [2021]; Li *et al.* [2022b]; Zhang *et al.* [2023]; Chen *et al.* [2024], use image-caption pairs as supervision to distill relational knowledge, enabling generalization to unseen concepts.

LLMs for Scene Graph Generation. With the rise of LLMs, several studies have attempted to synthesize scene graphs from natural language. LLM4SGG [Kim *et al.*, 2023] extracts relational triplets from both original and paraphrased captions using text-only LLMs. GPT4SGG [Chen *et al.*, 2023] goes a step further by using GPT-4 to generate scene graphs from dense region captions, improving contextual consistency and coverage. Meanwhile, Li *et al.* [2024] leverage vision-language models (VLMs) to produce scene graphs through image-to-text generation pipelines.

However, these caption-based or LLM-driven methods often exhibit limited accuracy, including incomplete object sets, and inconsistent relationship descriptions. These issues arise from the lack of structure in the generated outputs and the absence of mechanisms to refine the results according to scene-level constraints.

Reinforcement Learning (RL) for LLMs. Reinforcement learning (RL) has been increasingly adopted to enhance the reasoning capabilities of large models. Algorithms like Proximal Policy Optimization (PPO) [Schulman *et al.*, 2017] and Group Relative Policy Optimization (GRPO) [Shao *et al.*, 2024] guide models using reward signals instead of relying solely on maximum likelihood estimation. In the context of large language models, DeepSeek-R1 [Guo *et al.*, 2025] demonstrates that RL can significantly improve structured reasoning and planning.

In multimodal learning, however, RL remains underutilized for generating structured outputs. Our work addresses this by introducing rule-based reward functions at multiple levels—namely, node level, edge level, along with a format consistency reward. These signals promote the generation of meaningful and coherent scene graphs by explicitly evaluating alignment with ground-truth annotations.

3 Methodology

3.1 Preliminary

Scene Graph Generation (SGG). Scene graph generation (SGG) transforms an image I into a structured representation that captures both objects and their interactions. Specifically, SGG produces a directed graph $\mathcal{G} = (\mathcal{V}, \mathcal{E})$, where each node $v_i \in \mathcal{V}$ represents an object annotated with an object category c_i and a bounding box b_i. Each relationship triplet $e_{ij} \in \mathcal{E}$ captures the relationship between two nodes. The triplet is defined as $e_{ij} := \langle v_i,\, p_{ij},\, v_j \rangle$, where p_{ij} encodes the visual relationship between the subject v_i and the object v_j, such as spatial relations (*e.g.*, "on", "under") or interactive relations (*e.g.*, "riding", "holding"). Typically, SGG models decouple this task into two subtasks, namely object detection and relationship recognition, both optimized by maximizing the likelihood of the corresponding ground-truth labels given the image.

Reinforcement Learning with GRPO. Group Relative Policy Optimization (GRPO) is a online reinforcement learning algorithm introduced by DeepSeekMath [Shao *et al.*, 2024]. Unlike traditional methods such as PPO [Schulman *et al.*, 2017], which require an explicit critic network, GRPO instead compares groups of candiates to update the policy π_θ. Specifically, for each input query q, a set of candidate outputs $\{o_i\}_{i=1}^{G}$ is drawn from the previous policy $\pi^{\text{old}}(O|q)$, and the advantage of each candidate is computed relative to the group's average reward:

$$A_i = \frac{r_i - \text{mean}(\{r_1, \ldots, r_G\})}{\text{std}(\{r_1, \ldots, r_G\})}. \tag{1}$$

The policy parameters θ are updated by maximizing the following GRPO objective:

$$\begin{aligned} J_{\text{GRPO}}(\theta) = \mathbb{E}_{q\sim P(Q),\, \{o_i\}_{i=1}^{G} \sim \pi^{\text{old}}(O|q)} \Bigg[\frac{1}{G} \sum_{i=1}^{G} \Bigg(\min \Bigg(\frac{\pi_\theta(o_i|q)}{\pi^{\text{old}}(o_i|q)} A_i, \\ \text{clip}\Big(\frac{\pi_\theta(o_i|q)}{\pi^{\text{old}}(o_i|q)},\, 1-\epsilon,\, 1+\epsilon \Big) A_i \Bigg) - \beta\, D_{\text{KL}}\big(\pi_\theta \parallel \pi_{\text{ref}}\big) \Bigg], \end{aligned} \tag{2}$$

Here, ϵ and β are hyper-parameters. The first term uses a clipped probability ratio (as in PPO) to control the update magnitude, while the KL divergence regularizer $D_{\text{KL}}(\pi_\theta \parallel \pi_{\text{ref}})$ constrains the new policy π_θ to not deviate too much from a reference policy π_{ref}. This formulation, which combines a group-relative advantage, a clipping mechanism, and a KL divergence regularizer, stabilizes policy updates and improves training efficiency, demonstrating remarkable potential for enhancing the reasoning performance of LLMs such as DeepSeek R1 [Guo *et al.*, 2025].

3.2 Overview of R1-SGG

Graph Matching. Given an image and a text prompt, the M-LLM outputs a directed graph $\mathcal{G}_{\text{pred}}$, which needs to be matched to the ground-truth graph $\mathcal{G}$. To achieve this, we perform bipartite matching, as used in DETR [Carion *et al.*, 2020], to associate the prediction set $\{v_i\}_{i=1}^{M}$ with the ground-truth set $\{\tilde{v}_i\}_{i=1}^{N}$. The cost objective of the matching is formulated as:

$$\begin{aligned} \text{cost}(v_i, \tilde{v}_j) =& \lambda_1 \cdot (1.0 - \langle \texttt{Embedding}(c_i), \texttt{Embedding}(\tilde{c}_j) \rangle) \\ &+ \lambda_2 \cdot (1.0 - \text{IoU}(b_i, \tilde{b}_j)) + \lambda_3 \cdot ||b_i - \tilde{b}_j||_1, \end{aligned} \tag{3}$$

where $\langle \cdot, \cdot \rangle$ denotes cosine similarity, λ_1, λ_2 are weight factors, and `Embedding` is obtained via the NLP tool SpaCy. By solving the bipartite matching problem, we establish a one-to-one node matching between the predicted graph $\mathcal{G}_{\text{pred}}$ and the ground-truth graph $\mathcal{G}$. This matching enables the computation of rewards (see Section 3.3) to refine the M-LLM.

3.3 Rewards Definition

Format Reward. Following DeepSeek R1 [Guo *et al.*, 2025], we employ a format reward to ensure that the model's response adheres to the expected structure, specifically <think>$\cdots$</think><answer>$\cdots$</answer>. A reward of 1 is assigned if the response follows this format and the segment enclosed by <answer>$\cdots$</answer> contains both the keywords "object" and "relationships"; otherwise, the reward is 0. However, since small models such as Qwen/Qwen2-VL-2B-Instruct have limited ability to follow the system prompt, we relax this constraint by awarding a reward of 0.5 for responses that are formatted as valid JSON dictionaries, even if they do not strictly meet the original criteria.

Node-level Reward. For a predicted node v_i, the reward is defined as

$$\text{Reward}(v_i) = \begin{cases} \lambda_1 \cdot \langle \texttt{Embedding}(c_i), \texttt{Embedding}(\tilde{c}_j) \rangle & \\ \quad + \lambda_2 \cdot \text{IoU}(b_i, \tilde{b}_j) & \\ \quad + \lambda_3 \cdot \exp(-||b_i - \tilde{b}_j||_1), & \text{if } v_i \text{ and } \tilde{v}_j \text{ are matched,} \\ 0, & \text{otherwise.} \end{cases} \tag{4}$$

which is the linear combination of object category similarity and the IoU of bounding boxes. The total rewards of an image's prediction set $\{v_i\}_{i=1}^{M}$ is computed as

$$\text{Reward}(\{v_i\}_{i=1}^{M}) = \frac{1}{|\mathcal{V}_{\text{gt}}|} \sum_{i=1}^{M} \text{Reward}(v_i) \tag{5}$$

Edge-level Reward. For a predicted triplet $e_{ij} :=< v_i, p_{ij}, v_j >$, the reward is defined as

$$\text{Reward}(e_{ij}) = \begin{cases} \langle \texttt{Embedding}(v_i),\, \texttt{Embedding}(\tilde{v}_k) \rangle \cdot & \\ \langle \texttt{Embedding}(v_j),\, \texttt{Embedding}(\tilde{v}_l) \rangle \cdot & \\ \langle \texttt{Embedding}(p_{ij}),\, \texttt{Embedding}(p_{kl}) \rangle, & \text{if } v_i \text{ matches } \tilde{v}_k \\ & \quad \text{and } v_j \text{ matches } \tilde{v}_l, \\ 0, & \text{otherwise.} \end{cases} \tag{6}$$

Thereby, the reward of an image's predicted edge set is computed as

$$\text{Reward}(\{e_{ij}\}) = \frac{1}{|\mathcal{E}_{\text{gt}}|} \sum \text{Reward}(e_{ij}) \tag{7}$$

4 Experiments

4.1 Dataset and Experiment Setup

Dataset. We leverage the widely-used scene graph dataset, VG150 Xu *et al.* [2017], which consists of 150 object categories and 50 relationship categories. The training set contains $56,224$ image-graph pairs, while the validation set includes $5,000$ pairs. To prompt the M-LLM, we transform the image-graph pair using the template described in Table 1.

Evaluation. Following standard evaluation pipeline in SGG, we adopt the SGDET protocol to measure the model's ability to generate scene graphs.

Implementation Details. Our code is based on the `trl` library von Werra *et al.* [2020] and utilizes vLLM Kwon *et al.* [2023] to speed up sampling during reinforcement learning. For supervised fine-tuning (SFT), the model is trained for 3 epochs using 4x NVIDIA A100 (80GB) GPUs. For reinforcement learning (RL), the 2B model is trained for 1 epoch using 16x NVIDIA A100 (80GB) GPUs and the 7B model is trained for 1 epoch using 16x NVIDIA GH200 (120GB) GPUs.

4.2 How Well Do M-LLMs Reason About Visual Relationships?

We evaluate the visual relationship reasoning capabilities of open-source multimodal LLMs using a four-to-one Visual Question Answering (VQA) task. Each model is prompted with an image and a corresponding question. The used prompt template is:

Table 1: Prompting an M-LLM to generate scene graphs without providing predefined object classes or predicate types. The version with predefined classes and predicates is available in our code repository.

```
messages = [{ "role": "system", "content": " {system_prompt}" }, { "role": "user",
"content": f"""Generate a structured scene graph for an image of size using the following
format: “‘json { "objects": [ {"id": "object_name.number", "bbox": [x1, y1, x2, y2]}, ... ],
"relationships": [ {"subject": "object_name.number", "predicate": "relationship_type", "object":
"object_name.number"}, ... ] }“‘. ### **Guidelines:** - **Objects:** - Assign a unique ID
for each object using the format "object_name.number" (e.g., "person.1", "bike.2"). - Provide
its bounding box ‘[x1, y1, x2, y2]’ in integer pixel format. - Include all visible objects, even if
they have no relationships.
- **Relationships:** - Represent interactions accurately using "subject", "predicate", and "ob-
ject". - Omit relationships for orphan objects.
### **Example Output:** “‘json { "objects": [ {"id": "person.1", "bbox": [120, 200, 350,
700]}, {"id": "bike.2", "bbox": [100, 600, 400, 800]}, {"id": "helmet.3", "bbox": [150, 150,
280, 240]}, {"id": "tree.4", "bbox": [500, 100, 750, 700]} ], "relationships": [ {"subject": "per-
son.1", "predicate": "riding", "object": "bike.2"}, {"subject": "person.1", "predicate": "wearing",
"object": "helmet.3"} ] } “‘ Now, generate the complete scene graph for the provided image:
""" } ]
```

Table 2: Comparison of VQA on the VG150 validation set across various models and settings. Gains compared to the *Original Image* (1st row) are indicated in red. *"mask img."* refers to masking the entire image with random noise, *"mask obj."* refers to masking object regions with black pixels, *"wo cats."* refers to not providing object categories in the prompt, and *"wo box."* refers to not providing bounding boxes in the prompt.

	InstructBLIP 7B		**LLaVA v1.5 7B**		**LLaVA v1.6 7B**		**Qwen2VL 7B**	
	Acc	**mAcc**	**Acc**	**mAcc**	**Acc**	**mAcc**	**Acc**	**mAcc**
org. img.	2.26	1.94	45.75	45.61	28.69	29.17	53.74	53.35
mask img.	1.00 (-1.26)	1.04 (-0.90)	21.80 (-23.95)	21.61 (-24.00)	3.85 (-24.84)	3.95 (-25.22)	0.03 (-53.71)	0.02 (-53.33)
mask obj.	1.89 (-0.37)	1.86 (-0.08)	37.15 (-8.60)	37.16 (-8.45)	12.79 (-15.90)	13.22 (-15.95)	16.23 (-37.51)	16.82 (-36.53)
wo cats.	2.50 (+0.24)	2.38 (+0.44)	32.83 (-12.92)	32.68 (-12.93)	9.46 (-19.23)	10.11 (-19.06)	16.78 (-36.96)	18.06 (-35.29)
+ mask img.	0.97 (-1.29)	1.00 (-0.94)	15.41 (-30.34)	15.25 (-30.36)	0.01 (-28.68)	0.01 (-29.16)	0.18 (-53.56)	0.22 (-53.13)
+ mask obj.	1.75 (-0.51)	1.65 (-0.29)	27.91 (-17.84)	28.37 (-17.24)	3.26 (-25.43)	3.77 (-25.40)	4.67 (-49.07)	5.52 (-47.83)
wo box.	26.01 (+23.75)	25.93 (+23.99)	61.93 (+16.18)	61.32 (+15.71)	53.46 (+24.77)	52.10 (+22.93)	78.13 (+24.39)	77.10 (+23.75)
+ mask img.	10.14 (+7.88)	10.19 (+8.25)	36.26 (-9.49)	35.23 (-10.38)	11.47 (-17.22)	11.44 (-17.73)	0.01 (-53.73)	0.00 (-53.35)
+ mask obj.	19.26 (+17.00)	19.08 (+17.14)	54.23 (+8.48)	53.84 (+8.23)	33.46 (+4.77)	33.23 (+4.06)	40.26 (-13.48)	39.26 (-14.09)

```
Analyze the relationship between the object "{sub_name}" at
{sub_box} and the object "{obj_name}" at {obj_box} in an image
of size ({width}x{height}). The bounding boxes are in [x1,
y1, x2, y2] format. Choose the most appropriate relationship
from the following options: A) {choices[0]}; B) {choices[1]};
C) {choices[2]}; D) {choices[3]}.
```

We report Acc (accuracy over all questions) and mAcc (mean accuracy per image) in Table 2. The results reveal that many multimodal LLMs struggle with visual relationship reasoning. Moreover, the task exhibits a noticeable text bias, and the presence of bounding boxes can sometimes mislead the model's attention. As a simpler task compared to SGG, the poor performance suggests that directly applying multimodal LLMs to SGG may yield suboptimal results.

4.3 How Well do M-LLMs Generate Scene Graphs?

We report the performance under various settings in Table 3, which includes:

Table 3: SGDET Performance of `Qwen2VL-7B/2B-Instruct` models on the VG150 validation set.

Method	Params	Failure Rate (%)	AP50	R@20	R@50
w.o. predefined classes or predicates					
baseline	7B	47.26	6.75	0.84	0.84
zero-RL	7B	0.08 (-47.18)	13.97 (+7.22)	13.11 (+12.27)	13.11 (+12.27)
SFT	7B	40.16	13.66	9.15	9.15
SFT+RL	7B	0.04 (-40.12)	17.52 (+3.86)	20.16 (+11.01)	20.18 (+11.03)
baseline	2B	69.68	1.73	0.09	0.09
zero-RL	2B	0.06 (-69.62)	6.19 (+4.46)	4.34 (+4.25)	4.34 (+4.25)
SFT	2B	75.56	7.23	4.80	4.80
SFT+RL	2B	0.12 (-75.44)	16.58 (+9.35)	18.70 (13.90)	18.70 (13.90)
w. predefined classes & predicates					
baseline	7B	55.32	6.03	0.76	0.76
zero-RL	7B	0.08 (-55.24)	11.63 (+5.60)	10.67 (+9.91)	10.67 (+9.91)
SFT	7B	38.50	14.58	9.92	9.96
SFT+RL	7B	0.10 (-38.40)	18.72 (+4.14)	20.40 (+10.48)	20.47 (+10.51)
baseline	2B	56.56	2.31	0.17	0.17
zero-RL	2B	0.08 (-56.48)	8.03 (+5.72)	6.13 (+5.96)	6.13 (+5.96)
SFT	2B	73.80	7.81	5.13	5.13
SFT+RL	2B	0.28 (-73.52)	17.20 (+9.39)	18.82 (+13.69)	18.87 (+13.74)

- **Baseline**: Official models such as `Qwen/Qwen2-VL-7B-Instruct`[1] and `Qwen/Qwen2-VL-2B-Instruct`[2].
- **SFT**: Models fine-tuned using the standard supervised fine-tuning (SFT) paradigm.
- **Zero-RL**: Models trained with GRPO, without prior SFT on scene graph datasets.
- **SFT+RL**: Models trained with GRPO, initialized from SFT on scene graph datasets.

The results demonstrate that reinforcement learning (RL) significantly reduces the failure rate and enhances both object detection and relationship recognition. In contrast, supervised fine-tuning (SFT) alone results in a relatively high failure rate and limited performance improvements. As shown in Fig. 2, the failure rate rapidly declines to a very low level when using RL, whereas SFT continues to suffer from a high failure rate. Meanwhile, our experimental results suggest that predefined object classes or relationship categories are unnecessary, despite their potential to reduce the search space of M-LLMs.

5 Conclusion

This work explores the application of reinforcement learning (RL) to multimodal large language models (LLMs) for enhancing end-to-end scene graph generation (SGG). From the perspective of scene graphs, we design rule-based rewards, including node-level, edge-level, and format-based rewards. These reward formulations contribute to stable and effective policy optimization for scene graph tasks. We open-source our framework to foster further research and development in advancing multimodal LLMs for visual reasoning.

References

Nicolas Carion, Francisco Massa, Gabriel Synnaeve, Nicolas Usunier, Alexander Kirillov, and Sergey Zagoruyko. End-to-end object detection with transformers. In *ECCV*, pages 213–229. Springer, 2020.

Tianshui Chen, Weihao Yu, Riquan Chen, and Liang Lin. Knowledge-embedded routing network for scene graph generation. In *IEEE Conf. Comput. Vis. Pattern Recog.*, pages 6163–6171, 2019.

[1] `https://huggingface.co/Qwen/Qwen2-VL-7B-Instruct`

[2] `https://huggingface.co/Qwen/Qwen2-VL-2B-Instruct`

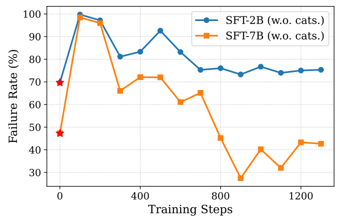

(a) Failure Rate vs Training Steps

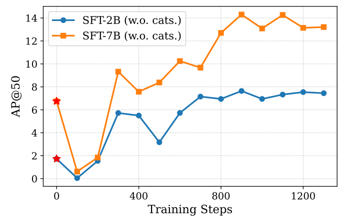

(b) AP@50 vs Training Steps

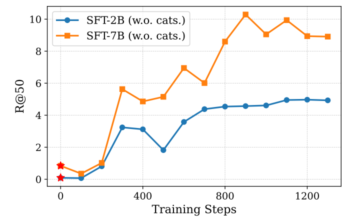

(c) R@50 vs Training Steps

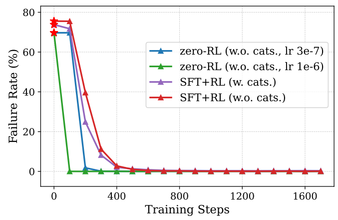

(d) Failure Rate vs Training Steps (2B)

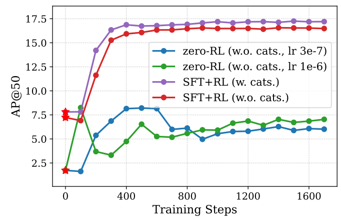

(e) AP@50 vs Training Steps (2B)

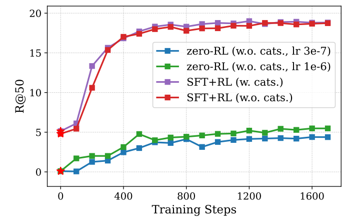

(f) R@50 vs Training Steps (2B)

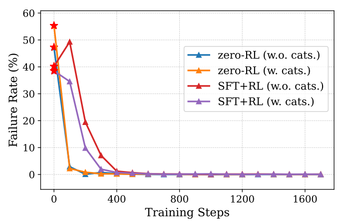

(g) Failure Rate vs Training Steps (7B)

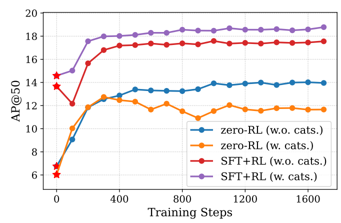

(h) AP@50 vs Training Steps (7B)

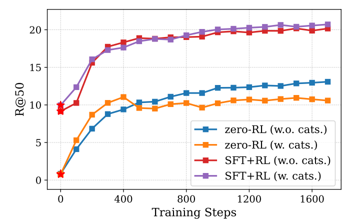

(i) R@50 vs Training Steps (7B)

Figure 2: Performance of `Qwen2VL-2B/7B-Instruct` during SFT / RL over training steps. For SFT, the model was trained with a batch size of 128 for 3 epochs. For RL, the model was trained for 1 epoch with a batch size of 32, and the group size of GRPO was set to 8. *w.o. cats.* refers to the setting without predefined object classes or predicate categories.

Zuyao Chen, Jinlin Wu, Zhen Lei, Zhaoxiang Zhang, and Changwen Chen. GPT4SGG: Synthesizing scene graphs from holistic and region-specific narratives. *arXiv preprint arXiv:2312.04314*, 2023.

Zuyao Chen, Jinlin Wu, Zhen Lei, Zhaoxiang Zhang, and Chang Wen Chen. Expanding scene graph boundaries: fully open-vocabulary scene graph generation via visual-concept alignment and retention. In *ECCV*, pages 108–124, 2024.

Yuren Cong, Michael Ying Yang, and Bodo Rosenhahn. Reltr: Relation transformer for scene graph generation. *IEEE Trans. Pattern Anal. Mach. Intell.*, 45(9):11169–11183, 2023.

Qiao Gu, Ali Kuwajerwala, Sacha Morin, Krishna Murthy Jatavallabhula, Bipasha Sen, Aditya Agarwal, Corban Rivera, William Paul, Kirsty Ellis, Rama Chellappa, et al. Conceptgraphs: Open-vocabulary 3d scene graphs for perception and planning. In *ICRA*, pages 5021–5028, 2024.

Daya Guo, Dejian Yang, Haowei Zhang, Junxiao Song, Ruoyu Zhang, Runxin Xu, Qihao Zhu, Shirong Ma, Peiyi Wang, Xiao Bi, et al. Deepseek-r1: Incentivizing reasoning capability in llms via reinforcement learning. *arXiv preprint arXiv:2501.12948*, 2025.

Justin Johnson, Ranjay Krishna, Michael Stark, Li-Jia Li, David Shamma, Michael Bernstein, and Li Fei-Fei. Image retrieval using scene graphs. In *CVPR*, pages 3668–3678, 2015.

Siddhesh Khandelwal and Leonid Sigal. Iterative scene graph generation. In Sanmi Koyejo, S. Mohamed, A. Agarwal, Danielle Belgrave, K. Cho, and A. Oh, editors, *Adv. Neural Inform. Process. Syst.*, 2022.

Kibum Kim, Kanghoon Yoon, Jaehyeong Jeon, Yeonjun In, Jinyoung Moon, Donghyun Kim, and Chanyoung Park. Llm4sgg: Large language model for weakly supervised scene graph generation. *arXiv e-prints*, pages arXiv–2310, 2023.

Harold W Kuhn. The hungarian method for the assignment problem. *Naval research logistics quarterly*, 2(1-2):83–97, 1955.

Woosuk Kwon, Zhuohan Li, Siyuan Zhuang, Ying Sheng, Lianmin Zheng, Cody Hao Yu, Joseph E. Gonzalez, Hao Zhang, and Ion Stoica. Efficient memory management for large language model serving with pagedattention. In *Proceedings of the ACM SIGOPS 29th Symposium on Operating Systems Principles*, 2023.

Yikang Li, Wanli Ouyang, Bolei Zhou, Kun Wang, and Xiaogang Wang. Scene graph generation from objects, phrases and region captions. In *ICCV*, pages 1270–1279, 2017.

Rongjie Li, Songyang Zhang, and Xuming He. Sgtr: End-to-end scene graph generation with transformer. In *IEEE Conf. Comput. Vis. Pattern Recog.*, pages 19464–19474, 2022.

Xingchen Li, Long Chen, Wenbo Ma, Yi Yang, and Jun Xiao. Integrating object-aware and interaction-aware knowledge for weakly supervised scene graph generation. In *ACMMM*, pages 4204–4213, 2022.

Rongjie Li, Songyang Zhang, Dahua Lin, Kai Chen, and Xuming He. From pixels to graphs: Open-vocabulary scene graph generation with vision-language models. In *CVPR*, pages 28076–28086, 2024.

Chen Lin, Shuai Zheng, Zhizhe Liu, Youru Li, Zhenfeng Zhu, and Yao Zhao. Sgt: Scene graph-guided transformer for surgical report generation. In *MICCAI*, pages 507–518, 2022.

Yang Miao, Francis Engelmann, Olga Vysotska, Federico Tombari, Marc Pollefeys, and Dániel Béla Baráth. SceneGraphLoc: Cross-Modal Coarse Visual Localization on 3D Scene Graphs. In *ECCV*, 2024.

Ege Özsoy, Evin Pınar Örnek, Ulrich Eck, Tobias Czempiel, Federico Tombari, and Nassir Navab. 4d-or: Semantic scene graphs for or domain modeling. In *MICCAI*, pages 475–485, 2022.

John Schulman, Filip Wolski, Prafulla Dhariwal, Alec Radford, and Oleg Klimov. Proximal policy optimization algorithms. *arXiv preprint arXiv:1707.06347*, 2017.

Zhihong Shao, Peiyi Wang, Qihao Zhu, Runxin Xu, Junxiao Song, Xiao Bi, Haowei Zhang, Mingchuan Zhang, YK Li, Y Wu, et al. Deepseekmath: Pushing the limits of mathematical reasoning in open language models. *arXiv preprint arXiv:2402.03300*, 2024.

Kaihua Tang, Hanwang Zhang, Baoyuan Wu, Wenhan Luo, and Wei Liu. Learning to compose dynamic tree structures for visual contexts. In *IEEE Conf. Comput. Vis. Pattern Recog.*, pages 6619–6628, 2019.

Leandro von Werra, Younes Belkada, Lewis Tunstall, Edward Beeching, Tristan Thrush, Nathan Lambert, Shengyi Huang, Kashif Rasul, and Quentin Gallouédec. Trl: Transformer reinforcement learning. `https://github.com/huggingface/trl`, 2020.

Danfei Xu, Yuke Zhu, Christopher B. Choy, and Li Fei-Fei. Scene graph generation by iterative message passing. In *CVPR*, pages 3097–3106, 2017.

Hang Yin, Xiuwei Xu, Zhenyu Wu, Jie Zhou, and Jiwen Lu. Sg-nav: Online 3d scene graph prompting for llm-based zero-shot object navigation. *NeurIPS*, 37:5285–5307, 2024.

Rowan Zellers, Mark Yatskar, Sam Thomson, and Yejin Choi. Neural motifs: Scene graph parsing with global context. In *IEEE Conf. Comput. Vis. Pattern Recog.*, pages 5831–5840, 2018.

Yong Zhang, Yingwei Pan, Ting Yao, Rui Huang, Tao Mei, and Chang Wen Chen. Learning to generate language-supervised and open-vocabulary scene graph using pre-trained visual-semantic space. In *CVPR*, pages 2915–2924, 2023.

Chenyangguang Zhang, Alexandros Delitzas, Fangjinhua Wang, Ruida Zhang, Xiangyang Ji, Marc Pollefeys, and Francis Engelmann. Open-vocabulary functional 3d scene graphs for real-world indoor spaces. In *CVPR*, 2025.

Yiwu Zhong, Jing Shi, Jianwei Yang, Chenliang Xu, and Yin Li. Learning to generate scene graph from natural language supervision. In *ICCV*, pages 1823–1834, 2021.

Yifeng Zhu, Jonathan Tremblay, Stan Birchfield, and Yuke Zhu. Hierarchical planning for long-horizon manipulation with geometric and symbolic scene graphs. In *ICRA*, pages 6541–6548, 2021.